Fertiliser Recovery from Source-Separated Urine via Membrane Bioreactor and Heat Localized Solar Evaporation

Jiawei Ren[a,b,1], Derek Hao[b,1], Jiaxi Jiang[b], Sherub Phuntsho[b], Stefano Freguia[c], Bing-Jie Ni[b], Pan Dai[d], Jing Guan[d], and Ho Kyong Shon[b,*]

[a] College of Architecture & Civil Engineering, Faculty of Urban Construction, Beijing University of Technology, Beijing 100124, China

[b] School of Civil and Environmental Engineering, University of Technology Sydney (UTS), City Campus, Broadway, NSW 2007, Australia

[c] Department of Chemical Engineering, The University of Melbourne, Parkville, VIC 3010 Australia

[d] Beijing Origin Water Membrane Technology Company Ltd., Beijing 101400, China

---

1: These authors contributed equally to this manuscript.

[*] Corresponding author: Tel.: (+61) 02 9514 2629; email: Hokyong.Shon-1@uts.edu.au

Abstract

Urine with its abundant macronutrients (N-P-K) is an ideal resource for the production of fertiliser. However, the odour and pathogens in the raw urine must be removed to meet the public acceptance of urine collection systems and to enable its safe reuse as a fertiliser. In this work, real urine was collected and treated through a pilot-scale gravity-driven membrane bioreactor (GDMBR) to remove the malodorous organics and to nitrify almost 50% of the ammonia into nitrate. The stablised urine was subsequently distilled via low-cost heat localized solar evaporation (HLSE) to produce a non-odorous solid fertiliser. The developed HLSE with a small footprint can attract bulk solution into a vertical insulated space and quickly heat it up to 68 °C within 1 hour. The HLSE process had vapor flux at 1.3 kg m^{-2} h^{-1} as well as high solar to vapor conversion efficiency at 87%. Based on the EDX mapping and XRD analysis, the generated crystals are mainly $NaNO_3$, NH_4Cl, NaCl, $NH_4H_2PO_4$ and K_2HPO_4, which are ideal nutrients for vegetation. Urine-derived fertilisers have better performance on the growth of basil than an all-purpose commercial fertilisers. Generally, the GDMBR-HLSE is a promising cost-effective and green technology for nutrients recovery from urine.

Keywords: source-separated urine; nutrient recovery; urine stabilization; membrane bioreactor; heat localised solar evaporation; urine fertiliser

1 Introduction

Human urine contains abundant nutrients like nitrogen (N), phosphate (P), potassium (K), calcium (Ca), magnesium (Mg) and sulphur (S), which make urine an attractive resource for their recovery as raw material for fertiliser production (Heinonen-Tanski et al., 2007; Volpin et al., 2018). Previous agricultural trials have proved that using urine as fertiliser can effectively increase crop yields and it is comparable with using synthetic fertilisers(Freguia et al., 2021). Meanwhile, after urine accounts for up to 80% NH_3-N in domestic wastewater but only around 1% of the volume of domestic wastewater, the cost of wastewater treatment will be greatly reduced if there is urine separation (Bisinella de Faria et al., 2015; Freguia et al., 2021; Jacquin et al., 2018; Larsen et al., 2009; Larsen et al., 2016; Maurer et al., 2003).

Since untreated urine contains some malodorous volatile scent chemicals (such as ammonia, methanethiol etc.) and harmful bacteria, it is hardly accepted by the public(Lienert and Larsen, 2010; Segrè Cohen et al., 2020). It is broadly agreed that urine should be processed into an odourless and aseptic fertiliser product before use. Moreover, the urea in raw urine is usually hydrolysed along the pipe network during collection and conveyance and causes high pH of about 9.2, with consequence release of ammonia (NH_3), struvite ($Mg(NH_4)PO_4 \cdot 6H_2O$) precipitation and pipeline blockages (Segrè Cohen et al., 2020; Udert et al., 2006). To solve these problems, a decentralized in-situ biological nitrification system is an ideal process to reduce pH, convert NH_3/NH_4^+ to NO_3^- for urine stabilization and degradation of the malodorous organics. With the increasing popularity of green buildings, the production of in-situ urine-source fertiliser is a better choice of nutrients for the growth of the in-situ vegetation(Kavvada et al., 2017). Apart from the irrigation of in-situ vegetation, produced urine fertiliser can also be concentrated to reduce the cost of conveyance and storage costs for vegetation in other places. Udert and Wächter (Udert and Wächter, 2012) investigated a biological urine oxidation process with a sequencing batch reactor (SBR) to reduce pH and remove organics, after which thermal distillation was used to produce highly concentrated fertiliser products. However, direct thermal distillation requires boiling the bulk solution at 100 °C or even 130 °C to obtain a higher concentration factor(Udert and Wächter, 2012). To further remove pathogenic bacteria and reduce energy consumption, Volpin et al (Volpin et al., 2020) investigated the use of a membrane bioreactor (MBR) followed by low temperature membrane-distillation (MD), which successfully produced a 20-time concentrated liquid fertiliser under a 50 °C operation.

Nevertheless, both conventional thermal distillation and low temperature membrane distillation are energy-intensive concentration processes. Alternatively, heat localized solar evaporation (HLSE) with natural solar energy was investigated in this study. HLSE is a state-of-the-art solar evaporation process, whereby solar irradiation can be efficiently absorbed in a localized area via a porous absorber to converge heat and bulk solution, which can significantly expedite generation of solar steam (Kashyap and Ghasemi, 2020). Xu et. al (Xu et al., 2020) studied an ultrahigh efficiency desalination via a thermally localized multistage solar still to harvest distilled water from sea water. Xia et.al (Xia et al., 2019) investigated a spatially isolating salt crystallisation process from seawater evaporation for continuous solar steam generation and salt harvesting. Most of the current studies in HLSE are focused on desalination for seawater recovery while the application of the heat localized solar evaporation process in nutrient recovery from urine is still an unexplored application.

In this study, in order to minimize the energy consumption, a gravity-driven membrane bioreactor (GDMBR) set-up was first applied to stabilize raw urine collected from waterless urinals at the University of Technology Sydney (UTS). The permeate after the treatment was dewatered using HLSE, which included a low-cost ink-printed capillary filter paper as the absorber for the liquid and energy absorption. Finally, the produced fertiliser was used to cultivate Basil (*Ocimum Basilicum*) via hydroponics. The produced urine-sourced fertiliser had a better performance than the check group from an all-purpose commercial fertiliser.

2 Methodology

2.1 Raw urine collection and storage

Raw urine was collected from around 40 male urinals at UTS Building 11, where the sewage drainage system has a urine-separated piping network. According to our previous experience and measurements(Volpin et al., 2020), urea is hydrolysed in the collection pipes by the time it reaches a collection tank at the bottom of the building. The urine was collected and stored in a 20 L plastic bottle and measured with electric conductivity (EC), pH, NH_3, dissolved organic carbon (DOC), anions (PO_4^{3-}, SO_4^{2-}, Cl^-, NO_2^- and NO_3^-) and cations (Na^+, K^+, Mg^{2+}, Ca^{2+}) (See Sec.2.5).

2.2 Urine stabilization via aerobic membrane bioreactor (MBR)

Urine stabilization by nitrification was conducted with a 100 L pilot-scale aerobic MBR reactor (Fig. 1), the effective reaction volume is 80L in this study. The biological sludge was originally taken from Central Park wastewater treatment plant (Sydney, NSW, Australia). Based on our previous experience, the pH was set at 6.2 to minimize the accumulation of NO_2^-. (Fumasoli et al., 2017) During the oxidation of NH_3 to NO_3^-, alkalinity was consumed, when the pH is lower than 6.2, hydrolysed urine was automatically pumped (BL7916-1 dosing pump, Hanna Instruments, Australia)) into the reactor to maintain pH. A commercial polyvinylidene fluoride (PVDF) corrugated microfiltration membrane module (FMBR-E-5) supplied by Beijing Originwater Technology was used. The nominal membrane pore size is 0.1 μm and the surface area is 0.06 m^2. Membrane module was soaked in the MBR and connected with a permeate tank to collect treated urine via gravity-driven filtration process. The hydrostatic height was kept at 60 cm to provide stable filtration driving force by ball float valve. Three air diffusers were evenly distributed in the reactor to supply fine bubble aeration, which can ensure the dissolved oxygen (DO) above 6 mg/L for biomass, air scrubbing for membrane and the full blending for reactor.

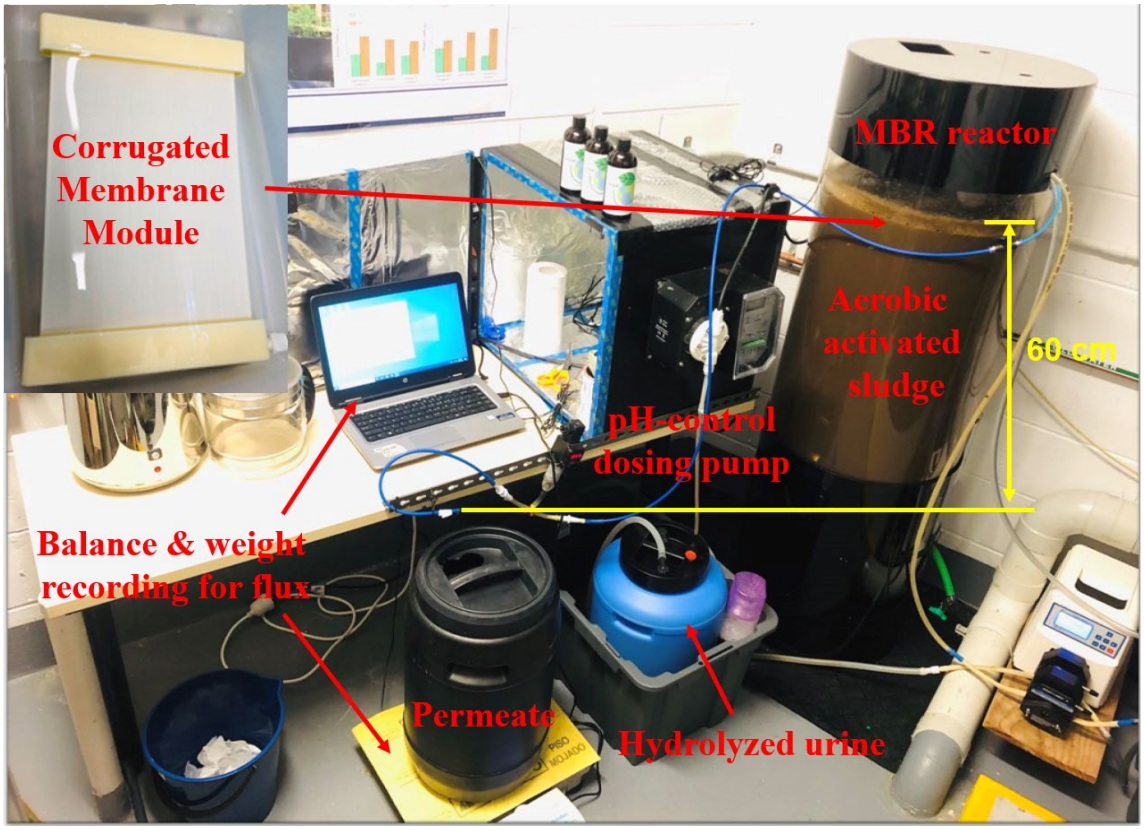

Fig.1 Pilot-scale MBR reactor for source-separated urine stablization

Theoretically, only 50% NH_3 can be converted to NO_3^- at most with only hydrolysed urine feeding(Udert and Wächter, 2012). The mixed liquor suspended solids (MLSS) of the reactor were maintained at 5 ± 1 g L^{-1} (solid retention time is around 200 d), which enable the MLSS/MLVSS ratio > 0.85. HRT varies from NH_3 concentration and membrane flux. After the MBR stabilized, the permeate was stored at 4℃ in preparation for the HLSE tests.

2.3 Heat localized solar evaporation (HLSE)

Heat localized solar evaporation (HLSE) process was selected for permeate concentration due to its zero energy consumption, low-cost and portable configuration (Lee et al., 2017).

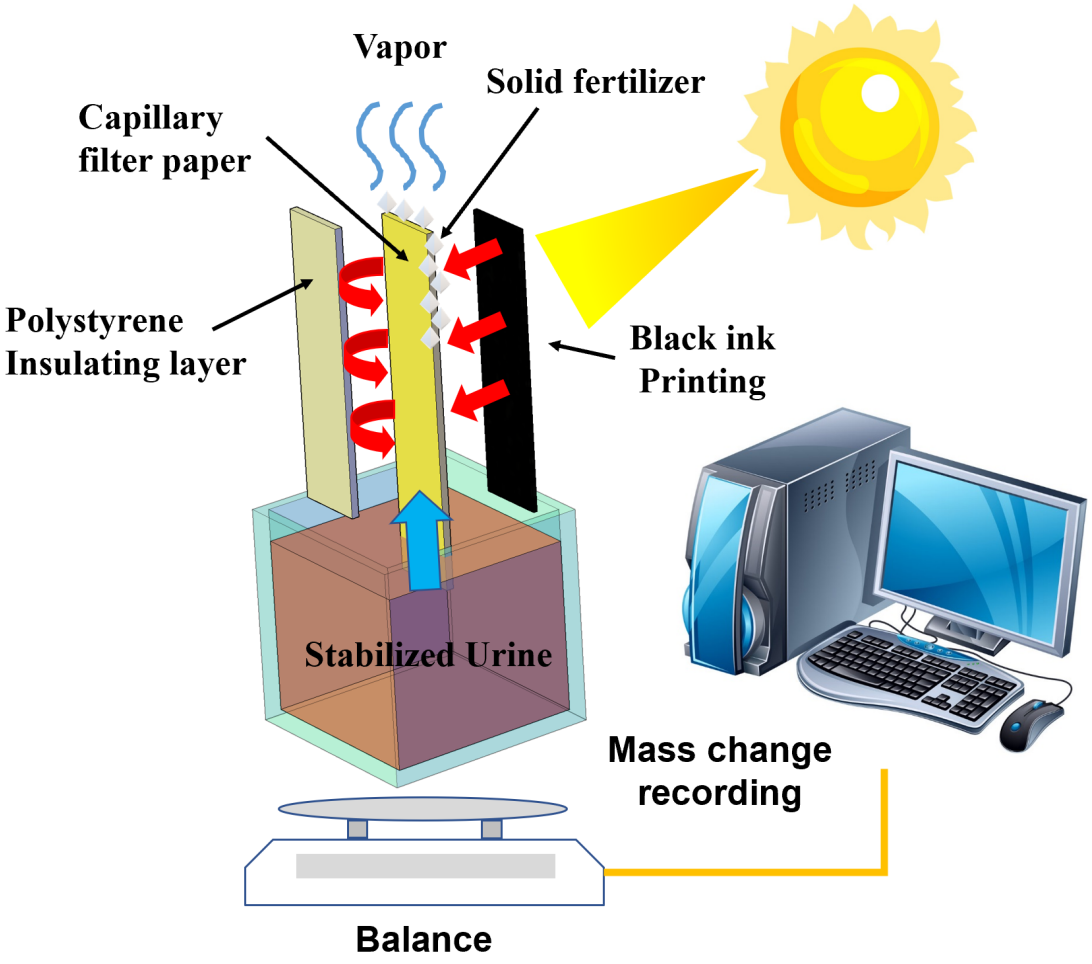

Fig.2 Schematic diagram of heat localized solar evaporation (HLSE) and absorber structures

Fig. 2 schematically shows the HLSE setup including a 3-layer absorber, a container, and a balance with a computer. In each experiment, 90 ml stabilized urine was collected from MBR permeate in a self-made quartz cubic container. The 3-layer absorber was vertically inserted in the container to minimize the footprint and heat loss. The middle layer of the absorber was

prepared by a 9 cm × 2 cm hydrophilic filter paper at 2mm thickness for capillary attraction. Commercial black ink (HP63 Black) is printed on the filter paper (HP DeskJet 2130 series 2) on one side as an adsorption layer to absorb solar radiation. On the other side, a polystyrene insulating layer was stuck to the filter paper to minimize thermal loss. The container was covered with a parafilm to avoid direct water evaporation from the solution surface. Subsequently, the absorber was exposed to continuous simulated solar irradiation for 24 h (the solar flux is controlled at 1000 w/m^2) via a solar simulator in a chamber with a ventilation system. The weight variation of the bulk solution was measured by a balance and recorded by a computer for water vapor flux calculation. After the process, the absorber was dried in oven at 60 °C overnight to quantify the solid fertiliser. The generated solid fertiliser powders were scraped off from the absorber after drying and collected in a sealed container filled with nitrogen gas. To investigate the evaporation performance of HLSE, permeate solutions in dark evaporation (DE), direct solar evaporation (DSE), heat localized solar evaporation with absorber in 1 piece (HLSE-1) and heat localized solar evaporation with the same absorber but cut into 2 pieces (HLSE-2) are compared in this study. The vapor flux is calculated as the followed Eq. 1.

$$\text{Vapor flux} = \triangle m / A \triangle t \qquad \text{(Eq. 1)}$$

Where the $\triangle m$ is the mass change of bulk solution, $\triangle t$ is the time change for the mass change, A is the effective irradiation area.

2.4 Hydroponic growth of basil with the urine-sourced fertiliser and commercial fertiliser

The urine-sourced solid fertiliser collected from the HLSE was used for hydroponic growth of basil (*Ocimum Basilicum*). The cultivation performance of the produced urine-source fertiliser, commercial fertiliser and DI water as blank solution was compared from seedling stage with a hydroponic method. Three basil seedlings purchased from flower market were rinsed and then cultivated in three conical flasks, where the flasks were filled with 250 mL urine-source fertiliser (2 g/L), commercial fertiliser (2 g/L) and DI water. The nutrients solutions were wasted and refilled per week. The temperature is ranging from 14 ± 3 °C to 30 ± 4 °C and humidity is 62 ± 15%. After 3 weeks growth, the leaves, roots and radicles are cut to compare the growth performance.

178 ### 2.5 Analytical measurements

179 #### 2.5.1 Water quality characterisation

180 Anions are measured using Ion Chromatography (IC, Thermo Fisher Scientific, USA) while
181 cations were measured using Inductively Coupled Plasma Mass Spectrometry (ICP-MS,
182 Agilent 7900, USA). NH_4^+ was measured via Spectroquant ammonia test kit. DOC was
183 measured by Analytikjena Multi N/C 2000. All the samples are filtered with a 0.45 μm before
184 measurement.

185 #### 2.5.2 Absorber and solid fertiliser characterization

186 Absorber and solid fertiliser surface morphology and element component analysis were
187 measured by scanning electron microscopy and energy dispersive X-ray spectrometry (SEM
188 and EDX, Zeiss Supra 55VP, Carl Zeiss AG) (Ren et al., 2019b). X-Ray diffraction (XRD,
189 Bruker D8 Discover) was carried out over Bragg angles ranging from 1° to 80° (Cu *Kα,* λ =
190 1.54059Å). A sessile drop method utilising Theta Lite 100 (Attension, Sweden) with built-in
191 software was used to analyse the contact angles of absorber before and after black ink
192 printing (Ren et al., 2019a). A water droplet around 5 μl was released from a needle tip onto
193 the filter paper surface. A motion camera was mounted to take photos at a rate of 12 frames
194 per second. Each sample was measured for three times and the average value was taken. The
195 solar absorbance test was scanned from 250 nm to 2500nm by Lambda 950.

196 ## 3 Results and Discussion

197 ### 3.1 Nitrification membrane bioreactor (MBR)

198 The MBR reactor was firstly started with 50 L running for 4 weeks and then upscaled to 80 L
199 and operated for 8 more weeks. For the 3-month operation, the sludge was gradually
200 acclimatised to the feed urine. The ratio of ammonia to nitrate conversion was stable at 48% -
201 50% after the last 6 weeks of operation (Fig. S1). The membrane flux was controlled at 3.8 –
202 14.8 LMH by monthly hydraulic cleaning (Fig. S2). An average HRT of 10 ± 5 days was
203 reached with an ammonia conversion rate of 230 ± 135 mg-N L^{-1} d^{-1}. After 3 months
204 operation, we collected the MBR permeate as the feed water for the subsequent HLSE test.
205 The components of the urine before and after MBR are listed in Table 1. The concentrations
206 of N, P and K in the raw urine are considerable at 2950, 280 and 1078 mg/L respectively,

which are similar as our previous bench-scale results (Volpin et al., 2020). After the nitrification process, ~ 95% TN remained in the permeate (the other 5% might be purged or consumed during the nitrification), ~ 50% of NH_4^+ was converted to NO_3^-, which makes the NH_4: NO_3^- ratio approximately 1:1. Meanwhile, the pH of the permeate decreased from 9.5 to 6.2, which is conducive to the stabilization of NH_4^+. The concentrations of Mg^{2+} and Ca^{2+} in the permeate are higher than those in the raw urine, which is probably because the re-dissolution of struvite ($Mg(NH_4)PO_4 \cdot 6H_2O$) and CaCO3 precipitated in the urine tank due to the change of pH. As the apparatus such as ICP-MS, IC required pre-filtration before measurement, struvite and CaCO3 as precipitants existed in the hydrolysed urine (alkaline ambience) were rejected by the filter, which caused the Mg^{2+} and Ca^{2+} concentrations to be lower in the untreated urine. The concentrations of P, K and other ions in the permeate are also the similar level as the untreated urine, which are expected in the urine-sourced fertiliser production.

Table 1. Characteristics and ionic composition of urine before and after MBR

	Unit	Raw untreated urine	Permeate
EC	[mS/cm]	30	27
pH	[-]	9.5	6
DOC	[mg/L]	778	140
NH_3/NH_4^+-N	[mg/L]	2950	1420
NO_3^--N	[mg/L]	n.d	1370
NO_2^--N	[mg/L]	n.d	n.d
Cl^-	[mg/L]	1860	1820
PO_4^{3-}-P	[mg/L]	280	285
SO_4^{2-}	[mg/L]	150	134
Na^+	[mg/L]	1739	1870
K^+	[mg/L]	1078	1170
Mg^{2+}	[mg/L]	0.35	12
Ca^{2+}	[mg/L]	6.27	31

3.2 Heat localized solar evaporation

3.2.1 Characterization of Absorber

The absorber is simply prepared with a commercial capillary filter paper and printed with blank ink (Fig. 3a). The absorbance of the absorbers ranging from 250 nm to 2500 nm was

measured. As shown in Fig. 3b, the raw filter paper had low absorbance between 250 to 1300 nm and weak absorbance between 1300 to 2500 nm. In contrast, the black filter paper had strong absorbance covering all the spectrum of UV-light, visible light and infrared light regions, which is consistent with the irradiation scope of solar light and proven to be an excellent absorber. In terms of the surface morphology, there is no big difference in fibre structure between the raw filter paper (Fig. 3c) and the black filter paper (Fig. 3d), but the ink-printed filter paper had smoother surface probably due to the printing process. The contact angle results indicated that after printing black ink, the filter paper surface transformed from hydrophilic (0 °, Fig. 3e) to hydrophobic (135.24 °, Fig. 3f). This is mainly because the black ink was oil-based. This property was designed to absorb solar energy from the hydrophobic front facet while the evaporation process was conducted on the hydrophilic side facets.

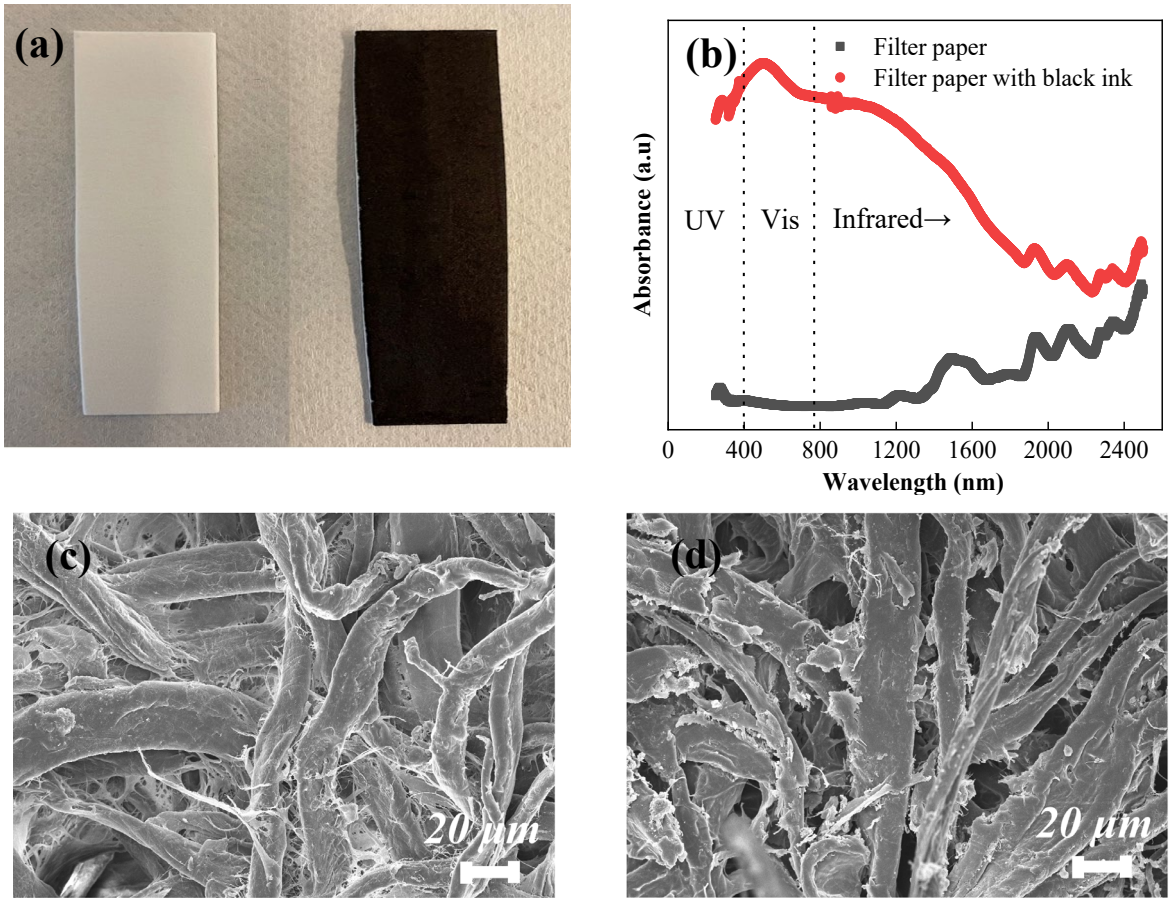

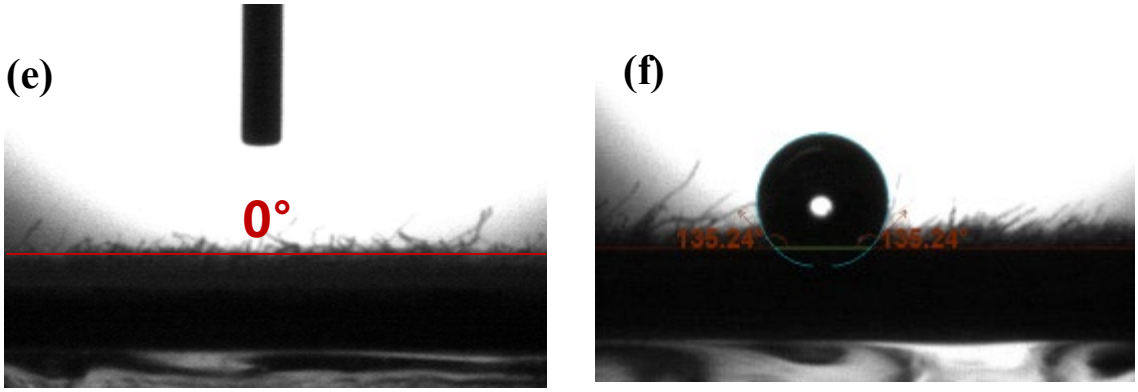

Fig. 3 Characterizations of the solar absorber. (a) Capillary filter paper and blank ink printed filter paper. (b) Absorbance of filter paper and black filter paper ranging from 250 to 2500 nm. (c)SEM image of raw filter paper (d) SEM image of black filter paper (e) Contact angle of raw filter paper (f) Contact angle of black filter paper

3.2.2 Performance of heat localized solar evaporation (HLSE)

To investigate the evaporation performance of HLSE, permeate solutions in dark evaporation (DE), direct solar evaporation (DSD), heat localized solar evaporation with 1 piece (HLSE-1), heat localized solar evaporation with 2 pieces (HLSE-2) are compared in this study. HLSE-1 and HLSE-2 had the same surface area for solar irradiation, but the absorber of HLSE-2 was cut into two pieces to increase extra lateral surface area for evaporation. As shown in Fig. 4a, the solution in the dark condition remains at room temperature (25 °C). When it comes to DSD, the solution temperature increased by 6°C within 0.5 h and then kept ~ 31°C till the end of the process. In contrast, the solution temperature of HLSE-1 and HLSE-2 increased significantly to 65 °C and 61 °C respectively within the first hour. Subsequently, they maintained 65~68 °C and 61~64 °C respectively during 1 to 12 h. After 12 h operation, both HLSE-1 and HLSE-2 temperature had a slightly decline from 65.4 to 63.5 °C and from 62.8 to 60.9 °C respectively. This is probably because the generation of solid fertiliser covered the surface and hindered the light absorption. Correspondingly, the mass changes and vapor flux had a consistent trend with the temperature variations. The solution mass of HLSE is lower than that of DE and SD. Specifically, DE, DSD, HLSE-1 and HLSE-2 evaporated 2.17, 6.67, 53.7 and 56.88 g respectively, during 24 h operation. Although HLSE-1 and HLSE-2 had the same front surface area for energy absorption, HLSE-2 had a larger surface area on the side for evaporation. In terms of the average vapor flux, HLSE-2 had the highest value at 1.33 kg m^{-2} h^{-1}, ~ 6% higher than HLSE-1, ~8.8 times higher than the DSD and ~26.6 times higher than the DE. The solar-to-vapor conversion efficiency η can be calculated from the vapor

flux and is given by Eq. 2(Xu et al., 2020),

$$\eta = \bar{m} h_t / q_{solar} \quad \text{(Eq. 2)}$$

where $\bar{m}$ is the vapor flux (g m^{-2} s^{-1}) under steady state, h_v is the enthalpy of water vaporization, q_{solar} is the input solar flux (1000 W m^{-2}). In this study, we used h_t = 2420, 2408, 2334 and 2322 kJ kg^{-1}, which corresponds to the latent heat at 25, 30, 60 and 65 °C, respectively. The solar-to-vapor conversion efficiency of SD, HLSE-1 and HLSE-2 are calculated as 9.3%, 81% and 87% respectively. Compared to the other water-based solar evaporation experiments, the vapor flux and solar-to-vapor conversion efficiency of HLSE-2 (1.33 kg m^{-2} h^{-1} and 87%) had the overwhelming performance.

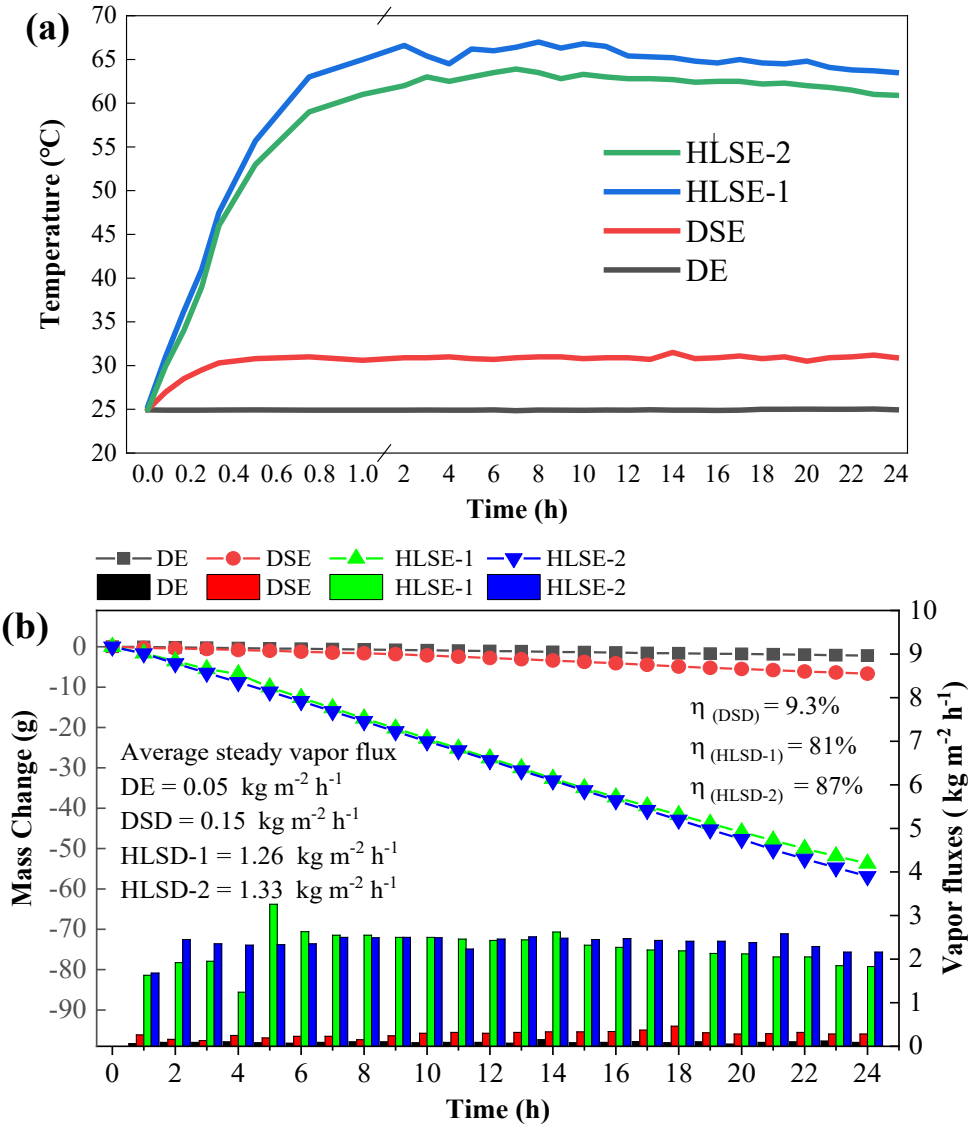

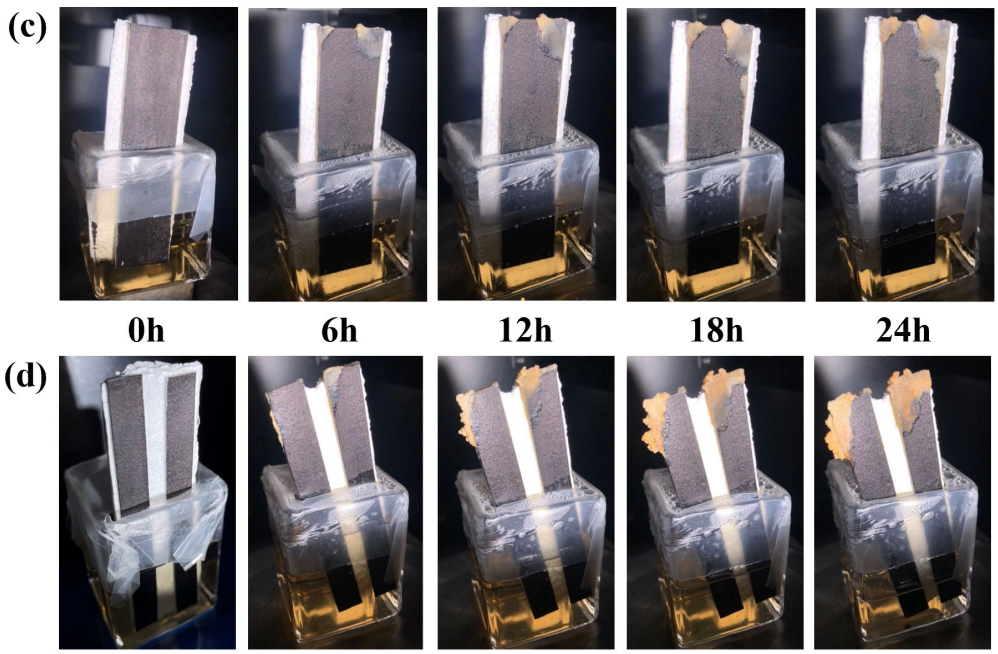

Fig. 4 Performance of the HLSE process. (a) Temperature evolution of dark evaporation (DE), solar evaporation (SD) and heat localized solar evaporation with 1 piece and 2 pieces (HLSE-1 and HLSE-2) (b) Mass changes, vapor fluxes and solar-to-vapor conversion efficiency of each evaporation test.
(c) Crystalization process of HLSE-1 and (d) HLSE-2

According to the images in Fig. 4c and 4d, it is observed that the crystals were initially generated on the corners of the absorber. Due to the front facet is the hydrophobic ink coating, solution was repulsed to the lateral side for the evaporation. As the corner had the most air-water interface area and the furthest distance from the bulk solution, the corner would have the optimal evaporation condition and nucleate earlier. With the accumulation of the crystals, the ambient surface area was gradually covered and absorbed less heat. As a result, crystallization interface was moving down along the lateral. After 24h, HLSE-2 generated 0.62 g solid fertiliser while HLSE-1generated 0.58 g solid fertiliser. Interestingly, due to the uneven generation of crystal and a slight change of solution water level, the absorber was slightly tilted. Therefore, crystals were also generated following the tilted position. This may be explained by the path of solution flow which was determined by effects of the capillary attraction and gravity.

3.2.3 Solid fertiliser components

The produced crystals are collected and dried in an oven at 60°C before use. The components

294 of the solid fertiliser are analysed by SEM-EDX and XRD.

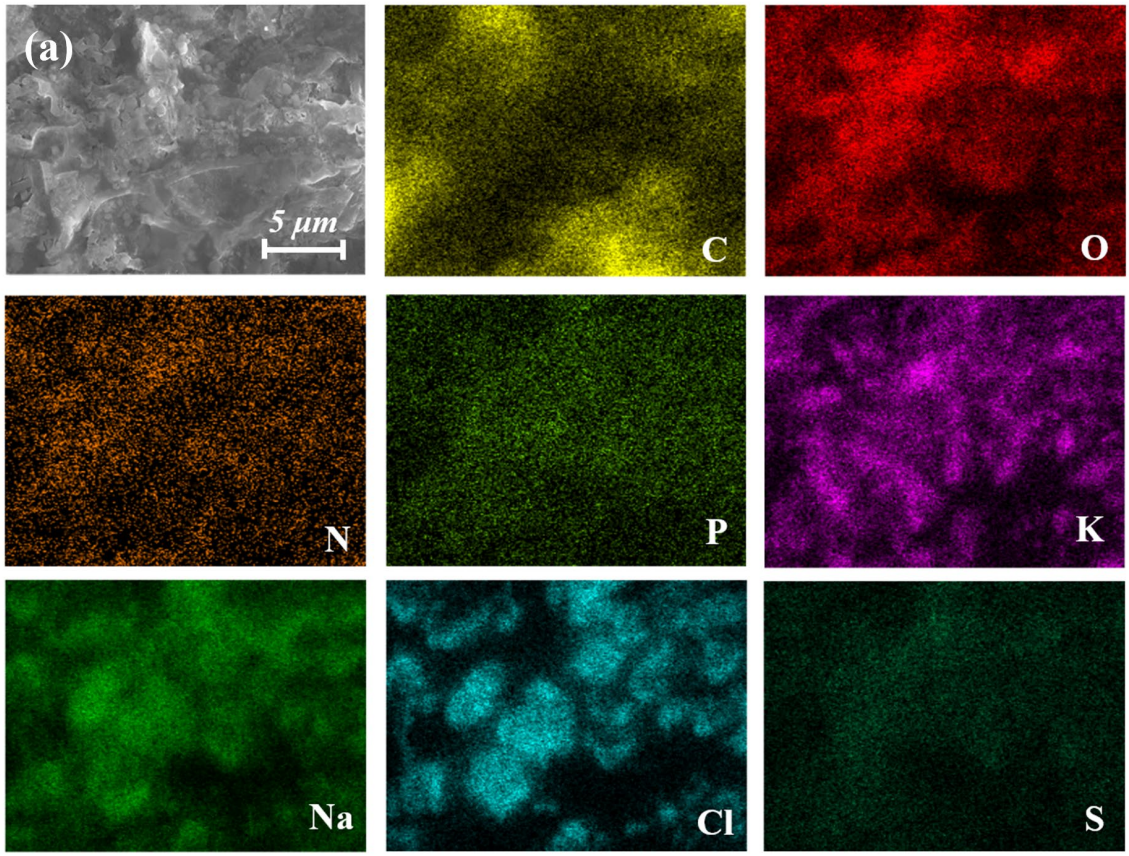

295

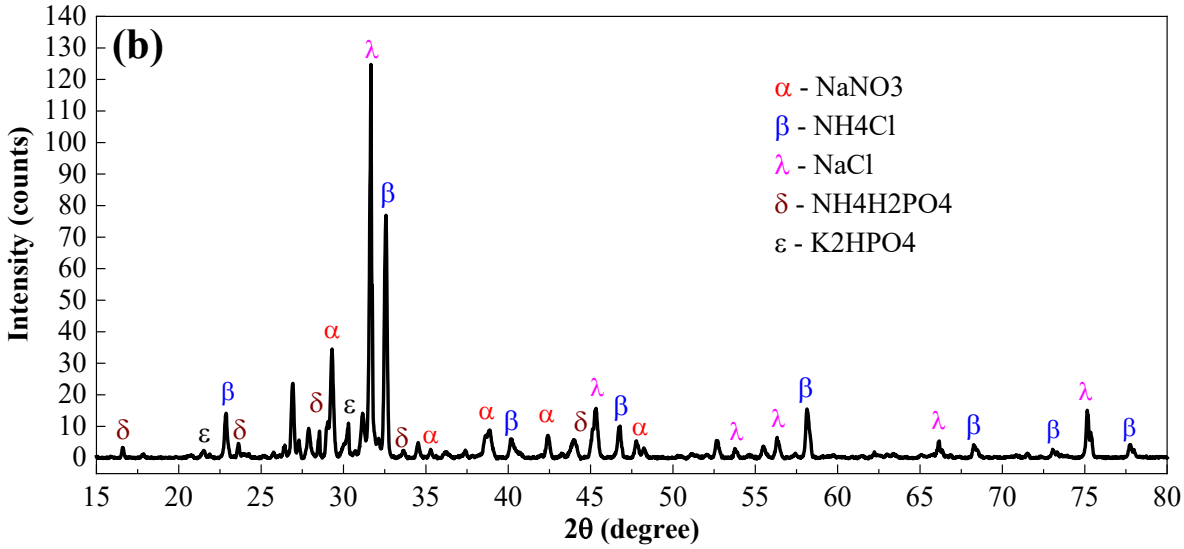

296

297 Fig. 5 Charaterizations of the solid fertiliser. (a) SEM-EDX images for elements mapping
298 analysis; (b) XRD for crystal type analysis

299 As shown in Fig. 5a, elements of C, O, N, P, K, Na, Cl, S are detected in the presented SEM
300 image area. N, P and K are the most primary elements that we are targeting in the nutrient

recovery from the urine permeate. According to the mapping images, N, P and K are well distributed in the crystals. The XRD result indicates that $NaNO_3$, NH_4Cl, NaCl, $NH_4H_2PO_4$ and K_2HPO_4 are the main crystals generated in the HLSE process, which is consistent with EDX mapping results. Specifically, the mapping distribution of Na and Cl proves the existence of NaCl crystal; the mapping distributions of K, O and P are consistent with K_2HPO_4 crystal. Since the N mapping includes both ammonium and nitrate, the N distribution was combined. $NaNO_3$, NH_4Cl, $NH_4H_2PO_4$ and K_2HPO_4 are typical components for commercial fertiliser. Therefore, the produced solid fertiliser is used for the subsequent hydroponics test.

3.3 Hydroponic test

To investigate the performance of the urine-sourced fertiliser, no fertiliser and commercial fertiliser (Brunnings, all-purpose NPK fertiliser) are also compared in the hydroponic tests. The components of the hydroponic medium after addition of urine-sourced fertiliser (2 g/L) and commercial fertiliser (2 g/L) are presented in Table 2. The primary macronutrients (N, P, K) in the urine-sourced fertiliser account for 15.5%, 1.9% and 9.2%, which means that the N and K are the main nutrients in the urine-sourced fertiliser. In contrast, the primary macronutrients (N, P, K) in the commercial fertiliser account for 7.8 %, 8.25 % and 9.6 %, which indicates that the ratio of N, P and K in the commercial fertiliser are more even. In terms of the secondary macronutrients, S, Ca, and Mg account for only 0.9%, 0.9% and 0.4% in urine-sourced fertiliser, which is much lower than those in commercial fertiliser (13.9%, 8% and 0.5%).

Table 2. Characteristics and ionic composition of urine-sourced fertiliser and the commercial fertiliser.

	Unit	Urine-sourced fertiliser	Commercial fertiliser
EC	[mS/cm]	2.9	3.2
pH	[-]	5.90	6.20
DOC	[mg/L]	4	1
NH_3/NH_4^+—N	[mg/L]	168	156
NO_3^-N	[mg/L]	141	<1
NO_2^-N	[mg/L]	-	-
Cl^-	[mg/L]	264.3	74
PO_4^{3-}P	[mg/L]	38	165
SO_4^{2-}	[mg/L]	17.4	278
Na^+	[mg/L]	220	18
K^+	[mg/L]	184.3	192

Mg^{2+}	[mg/L]	8.48	11
Ca^{2+}	[mg/L]	17.46	160

Fig. 6a and Fig. 6b presented the 3-week growth of the basils in DI water, urine-sourced fertiliser, and commercial fertiliser. Clearly, the urine-sourced fertiliser grew best with a larger leaf size, longer stems and roots, and more robust colour. On the contrary, the basil grew in DI water with the smallest size of leaf, stem and roots, and yellow pattern was apparently unhealthy due to lack of nutrients. The commercial fertiliser falls in between with a green colour but medium size leaves, stems, and roots. Specifically, the leaf weight of the basil grown in urine-sourced fertiliser (196.6 ± 48.4 mg) was ~ 2.4 times the figure for that in commercial fertiliser (80.3 ± 23.7 mg) and ~ 3.7 times the figure for that in DI water (51.8 ± 17.5 mg). The leaf area of basil grew in urine-sourced fertiliser (11.4 ± 2.9 cm^2) was ~ 2.3 times the figure for commercial fertiliser (4.9 ± 1.6 cm^2) and ~ 4.2 times the figure for DI water (2.7 ± 0.7 cm^2). Meanwhile, the stem height and diameter of the basil grew in urine-sourced fertiliser (18 ± 1.5 and 0.35 ± 0.05 cm) are more than twice in commercial fertiliser (8.5 ± 0.8 and 0.17 ± 0.03 cm) and in DI water (7.5 ± 0.7 and 0.15 ± 0.02 cm). The main reason why the urine-based fertiliser had a better performance in basil growth is probably because of a higher ratio of N. N as the primary macronutrient plays the most significant role in leaf and stem growth, especially for herbs in the seedling stage. Although commercial fertiliser had higher concentrations of other nutrients (P, S and Ca), N as the predominant nutrient is only half of the concentration in urine-sourced fertiliser.

The basil root in urine-source fertiliser also had the highest weight (5.5 ± 2.3 mg) and length (4 ± 2.8 cm) while commercial fertiliser had lower weight (2.5 ± 1.5 mg) and length (2.7 ± 1.6 cm) which are similarly as those in DI water (2.8 ± 1.3 mg and 3 ± 1.5 cm). This is mainly because the presence of NO_3^- in urine-sourced fertiliser contributes to the growth of roots (Kristensen and Thorup-Kristensen, 2004). Besides, some other micronutrients may also contribute to the growth of basil.

We also conducted two more hydroponic tests to compare the liquid urine-sourced fertiliser with another commercial liquid fertiliser (Power Feed) for the growth of both basil and coriander as reference (Fig. S3). The results indicate that the produced urine-sourced fertiliser had a comparable performance with commercial fertiliser. More related results will be discussed in the future work.

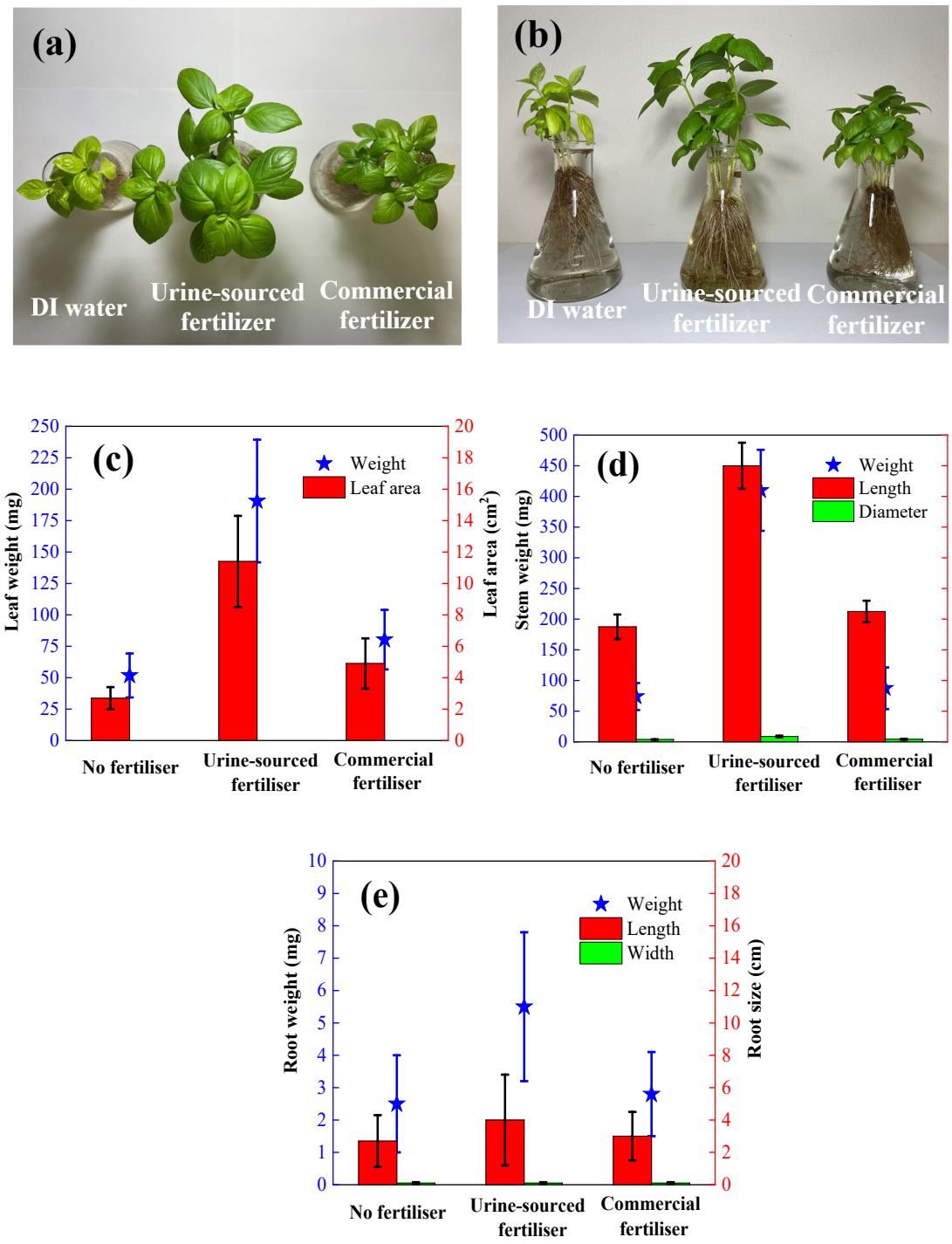

Fig. 6 Hydroponics tests of DI water, urine-sourced fertiliser and commercial fertiliser for 3 weeks from seedling stage. (a) top view of the basil growth performances ; (b) front view of the basil growth performances ; (c) Leaf weight and size of each sample ; (d) Stem weight and size of each sample; (d) Root weight and size of each sample.

4 Conclusions

In this study, source-separated urine was stabilized using gravity-driven MBR and then dewatered through HLSE to produce solid fertiliser, which was tested to grow Basil by hydroponics. The MBR reactor successfully converted ~ 50% of NH_3 to NO_3^- and removed malodorous smell. The nitrified urine with a low pH of 6 was stabilized and managed to generate crystals via HLSE process. The developed HLSE with a very low-cost absorber can attract bulk solution into a vertical insulated space and heat the solution up to 68 °C within 1 h to distil water and harvest crystals simultaneously. The HLSE method achieved a high vapor flux of 1.33 kg m^{-2} h^{-1} and overwhelming evaporation efficiency at 87%. The generated crystals, mainly including $NaNO_3$, NH_4Cl, NH_4H_2PO4 and K_2HPO_4, could be applied as solid fertiliser for basil growth. Its performance showed comparable adaptation for basil growth to an all-purpose commercial fertiliser. Finally, the GDMBR-HLSE as a cost-effective green technology is probably a promising field in nutrients recovery from urine. Further studies, such as simultaneous recoveries of nutrients and water, continuous production of crystals, the optimization and regeneration of absorbers, life cycle assessment for the whole process are being investigated and will be reported in the future work.

Acknowledgements

This research was supported by the ARC Industrial Transformation Research Hub (IH170100009) and code NRF-2017M1A2A2047369 by National Research Foundation of Korea, Republic of Korea.

386 **References:**

387 Bisinella de Faria, A.B., Spérandio, M., Ahmadi, A. and Tiruta-Barna, L. 2015.
388 Evaluation of new alternatives in wastewater treatment plants based on dynamic
389 modelling and life cycle assessment (DM-LCA). Water Research 84, 99-111.
390 Freguia, S., Sharma, K., Benichou, O., Mulliss, M. and Shon, H. 2021. Sustainable
391 engineering of sewers and sewage treatment plants for scenarios with urine diversion.
392 Journal of Hazardous Materials, 125609.
393 Fumasoli, A., Bürgmann, H., Weissbrodt, D.G., Wells, G.F., Beck, K., Mohn, J., Morgenroth,
394 E. and Udert, K.M. 2017. Growth of Nitrosococcus-Related Ammonia Oxidizing
395 Bacteria Coincides with Extremely Low pH Values in Wastewater with High
396 Ammonia Content. Environmental Science & Technology 51(12), 6857-6866.
397 Heinonen-Tanski, H., Sjöblom, A., Fabritius, H. and Karinen, P. 2007. Pure human urine
398 is a good fertiliser for cucumbers. Bioresource technology 98(1), 214-217.
399 Jacquin, C., Monnot, M., Hamza, R., Kouadio, Y., Zaviska, F., Merle, T., Lesage, G. and
400 Héran, M. 2018. Link between dissolved organic matter transformation and
401 process performance in a membrane bioreactor for urinary nitrogen stabilization.
402 Environmental Science: Water Research & Technology 4(6), 806-819.
403 Kashyap, V. and Ghasemi, H. 2020. Solar heat localization: concept and emerging
404 applications. Journal of Materials Chemistry A 8(15), 7035-7065.
405 Kavvada, O., Tarpeh, W.A., Horvath, A. and Nelson, K.L. 2017. Life-cycle cost and
406 environmental assessment of decentralized nitrogen recovery using ion exchange
407 from source-separated urine through spatial modeling. Environmental science &
408 technology 51(21), 12061-12071.
409 Kristensen, H.L. and Thorup-Kristensen, K. 2004. Root growth and nitrate uptake of three
410 different catch crops in deep soil layers. Soil Science Society of America Journal
411 68(2), 529-537.
412 Larsen, T.A., Alder, A.C., Eggen, R.I.L., Maurer, M. and Lienert, J. 2009. Source
413 separation: Will we see a paradigm shift in wastewater handling? Environmental
414 Science and Technology 43(16), 6121-6125.
415 Larsen, T.A., Hoffmann, S., Lüthi, C., Truffer, B. and Maurer, M. 2016. Emerging
416 solutions to the water challenges of an urbanizing world. Science 352(6288), 928-933.
417 Lee, J.-G., Alsaadi, A.S., Karam, A.M., Francis, L., Soukane, S. and Ghaffour, N. 2017.
418 Total water production capacity inversion phenomenon in multi-stage direct contact
419 membrane distillation: A theoretical study. Journal of Membrane Science 544,
420 126-134.
421 Lienert, J. and Larsen, T.A. 2010. High acceptance of urine source separation in seven
422 European countries: a review. Environmental science & technology 44(2), 556-566.
423 Maurer, M., Schwegler, P. and Larsen, T.A. 2003 Nutrients in urine: Energetic aspects of
424 removal and recovery, pp. 37-46.
425 Ren, J., Woo, Y.C., Yao, M., Lim, S., Tijing, L.D. and Shon, H.K. 2019a. Nanoscale
426 zero-valent iron (nZVI) immobilization onto graphene oxide (GO)-incorporated
427 electrospun polyvinylidene fluoride (PVDF) nanofiber membrane for groundwater
428 remediation via gravity-driven membrane filtration. Science of the total environment
429 688, 787-796.
430 Ren, J., Yao, M., Woo, Y.C., Tijing, L.D., Kim, J.-H. and Shon, H.K. 2019b. Recyclable
431 nanoscale zerovalent iron (nZVI)-immobilized electrospun nanofiber composites with
432 improved mechanical strength for groundwater remediation. Composites Part B:
433 Engineering 171, 339-346.

Segrè Cohen, A., Love, N.G., Nace, K.K. and Árvai, J. 2020. Consumers' acceptance of agricultural fertilizers derived from diverted and recycled human urine. Environmental science & technology 54(8), 5297-5305.

Udert, K., Larsen, T.A. and Gujer, W. 2006. Fate of major compounds in source-separated urine. Water Science and Technology 54(11-12), 413-420.

Udert, K. and Wächter, M. 2012. Complete nutrient recovery from source-separated urine by nitrification and distillation. Water research 46(2), 453-464.

Volpin, F., Chekli, L., Phuntsho, S., Cho, J., Ghaffour, N., Vrouwenvelder, J.S. and Shon, H.K. 2018. Simultaneous phosphorous and nitrogen recovery from source-separated urine: A novel application for fertiliser drawn forward osmosis. Chemosphere 203, 482-489.

Volpin, F., Jiang, J., El Saliby, I., Preire, M., Lim, S., Johir, M.A.H., Cho, J., Han, D.S., Phuntsho, S. and Shon, H.K. 2020. Sanitation and dewatering of human urine via membrane bioreactor and membrane distillation and its reuse for fertigation. Journal of Cleaner Production 270, 122390.

Xia, Y., Hou, Q., Jubaer, H., Li, Y., Kang, Y., Yuan, S., Liu, H., Woo, M.W., Zhang, L. and Gao, L. 2019. Spatially isolating salt crystallisation from water evaporation for continuous solar steam generation and salt harvesting. Energy & Environmental Science 12(6), 1840-1847.

Xu, Z., Zhang, L., Zhao, L., Li, B., Bhatia, B., Wang, C., Wilke, K.L., Song, Y., Labban, O. and Lienhard, J.H. 2020. Ultrahigh-efficiency desalination via a thermally-localized multistage solar still. Energy & Environmental Science 13(3), 830-839.